DNA Nanostructures

DOI: 10.1002/ange.201403455

Self-Assembly of DNA–Oligo(*p*-phenylene-ethynylene) Hybrid Amphiphiles into Surface-Engineered Vesicles with Enhanced Emission**

*Shine K. Albert, Hari Veera Prasad Thelu, Murali Golla, Nithiyanandan Krishnan, Soma Chaudhary, and Reji Varghese**

Dedicated to Professor M. V. George on his 86th birthday

Abstract: *Surface-addressable nanostructures of linearly π-conjugated molecules play a crucial role in the emerging field of nanoelectronics. Herein, by using DNA as the hydrophilic segment, we demonstrate a solid-phase "click" chemistry approach for the synthesis of a series of DNA–chromophore hybrid amphiphiles and report their reversible self-assembly into surface-engineered vesicles with enhanced emission. DNA-directed surface addressability of the vesicles was demonstrated through the integration of gold nanoparticles onto the surface of the vesicles by sequence-specific DNA hybridization. This system could be converted to a supramolecular light-harvesting antenna by integrating suitable FRET acceptors onto the surface of the nanostructures. The general nature of the synthesis, surface addressability, and biocompatibility of the resulting nanostructures offer great promises for nanoelectronics, energy, and biomedical applications.*

Crafting of surface-engineered nanostructures of π-conjugated molecules with promising optical properties is extremely important for molecular and supramolecular electronics.[1,2] This is primarily because such nanostructures allow their exact positioning at desired location, which is a great challenge in nanoelectronics. Furthermore, surface-engineered chromophoric assemblies may be used as supramolecular templates for the organization of other functional molecules, and thus provide a unique opportunity to study their electronic interaction with chromophoric stacks. DNA has proven to be an ideal candidate in the creation of surface-addressable nanostructures by making use of the principles of DNA nanotechnology.[3,4] One common strategy to obtain chromophoric assemblies using DNA is through the covalent incorporation of multiple chromophores into DNA.[5] Another approach involves DNA-templated non-covalent assembly of chromophores along the structural scaffold of DNA.[6] Despite these approaches providing an ideal platform for the helical organization of chromophores, creation of surface-engineered nanostructures of diverse morphology is challenging.

Very recently, DNA-based amphiphiles have emerged as a promising candidate in the creation of responsive nanostructures of distinct morphology.[7] The most remarkable structural features of this class of nanomaterials are surface addressability, biocompatibility, and morphology tunability due to the presence of a dense array of DNA molecules on their surface. More importantly, such nanostructures have shown potential applications in many fields ranging from biomedicine[8] to material sciences.[9] Hydrophobic moieties derived from different classes of non-chromophores including polymers,[10] dendrimers,[11] and long hydrocarbon chains[12] have been used for the design of DNA amphiphiles, but chromophoric systems are less exploited.[9a,13] Motivated from these reports, we envisioned that the covalent conjugation of a short DNA (10-mer) into a hydrophobic chromophore would generate a new class of DNA–chromophore amphiphile, and their self-assembly would offer a unique class of DNA-directed surface-engineered chromophoric assemblies. Unlike non-chromophoric DNA amphiphiles, the large π-surface of chromophore-based DNA amphiphiles can greatly enhance the self-assembly propensity through strong π–π stacking interaction, and thereby allows modulation of optical properties of the resulting nanostructures.

Among the different classes of π-conjugated chromophores, self-assembly of oligo(*p*-phenylene-ethynylene)s (OPEs) have received considerable attention as molecular wires for nanoelectronics.[14] Gothelf and Yan et al. have extensively studied non-amphiphilic DNA–OPE conjugates for the DNA-programmed assembly and synthesis of OPE-based molecular wires.[15,16] Non-amphiphilic DNA–OPE hybrids have also been used for the assembly of DNA-directed cage-like structures[17] and for the design of molecular-beacon-based DNA sensors.[18] However, amphiphilic DNA–OPE conjugate has not yet been studied. Herein, we report the synthesis of a series of DNA–OPE hybrid amphiphiles, and their reversible self-assembly in aqueous media into fluorescent nano- to microvesicles with tunable emission. Vesicles are self-assembled through the hydrophobic and π–π stacking interactions of OPEs, which constitute the membrane of the vesicle, whereas the hydro-

[*] S. K. Albert, H. V. P. Thelu, M. Golla, N. Krishnan, S. Chaudhary, Dr. R. Varghese
School of Chemistry, Indian Institute of Science Education and Research-Thiruvananthapuram (IISER-TVM)
CET campus, Trivandrum-695016 (India)
E-mail: reji@iisertvm.ac.in

[**] R.V. is grateful to the DST for a Ramanujan Fellowship. We thank CSIR-NIIST for TEM experiments. We thank Dr. Subi J. George, JNCASR, for HR-MS analyses and Dr. Mahesh Hariharan for helpful discussion.

Supporting information for this article is available on the WWW under http://dx.doi.org/10.1002/anie.201403455.

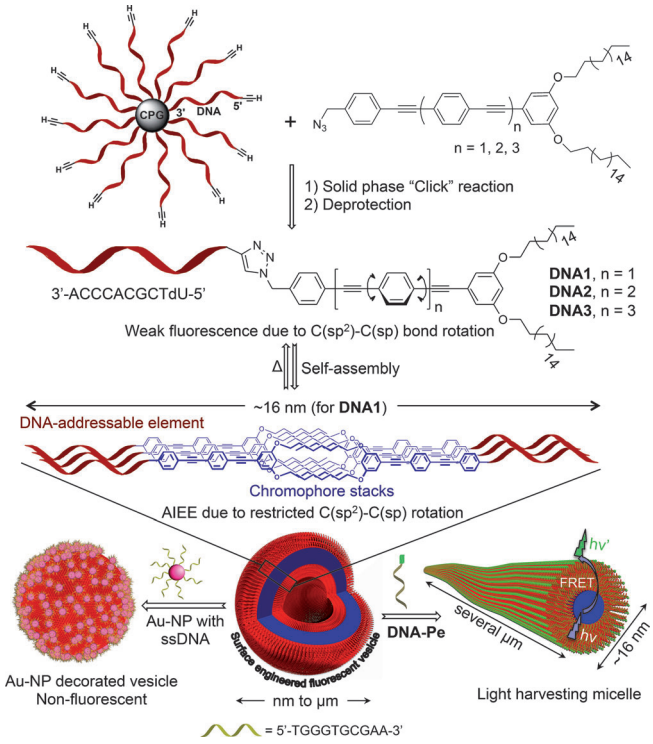

Scheme 1. Solid-phase "click" chemistry approach for the synthesis of **DNA1–3** amphiphiles and their reversible self-assembly into surface-engineered vesicles with enhanced emission. Bottom left: Surface decoration of vesicles with Au-NPs; bottom right: a fluorophore for the design of light harvesting antennae through sequence-specific DNA duplex formation.

philic DNA is exposed to the polar medium on either side of the membrane as shown in Scheme 1. Strong aggregation-induced enhanced emission (AIEE) is observed for the vesicles due to the restricted rotation of $C(sp^2)$–C(sp) bonds of the OPE segment of the amphiphiles. Since vesicles are surface-engineered with hydrophilic DNA, we explore the Watson–Crick base-pairing property of DNA for the reversible surface modification of the vesicles with other functional molecules such as gold nanoparticles (Au-NPs). We also demonstrate the potential of our system in the designing of a supramolecular light-harvesting antenna through the integration of suitable Förster resonance energy transfer (FRET) acceptors onto the surface of the vesicle (Scheme 1).

For the synthesis of DNA–OPE hybrid amphiphiles (**DNA1–3**) we adopted a solid phase "click" chemistry approach (Scheme 1);[19] the synthesis details are provided in the Supporting Information (SI). The only structural difference between **DNA1–3** is the difference in the conjugation length of OPE segment, which is systematically increased from **DNA1** to **DNA3** by increasing the number of OPE repeating units keeping the DNA sequence unchanged. This structural modification was intended for tuning the optical properties of the resulting nanostructures as a function of the conjugation length of the OPE segment.

Typically, self-assembly was performed by heating the amphiphiles (1 μM) in Tris buffer (50 mM, pH 7.4) at 90 °C for 5 min and then allowing to cool to room temperature. UV/Vis absorption spectra of self-assembled solutions of **DNA1–3** revealed the characteristic absorption peaks of DNA (λ_{max} = 260 nm) and π-stacked OPEs (λ_{max} = 320 nm, 335 nm and 350 nm for **DNA1**, **DNA2**, and **DNA3**, respectively, SI, Figure S2). They also displayed induced circular dichroism (ICD) signals in the absorption region of OPEs due to the transfer of molecular chirality of sugar units of DNA into the chromophoric stacks (SI, Figure S3).[14b,20] Dynamic light scattering (DLS) analysis of self-assembled solution of **DNA1** shows bimodal distribution of spherical aggregates, whereas **DNA2** and **DNA3** self-assemblies show unimodal distribution of spherical aggregates. The observed average diameters of **DNA1–3** spheres are 451 nm (major peak, σ = 0.57), 500 nm (σ = 0.22), and 795 nm (σ = 0.22), respectively (Figure 1 a–c). Field emission scanning electron microscopy

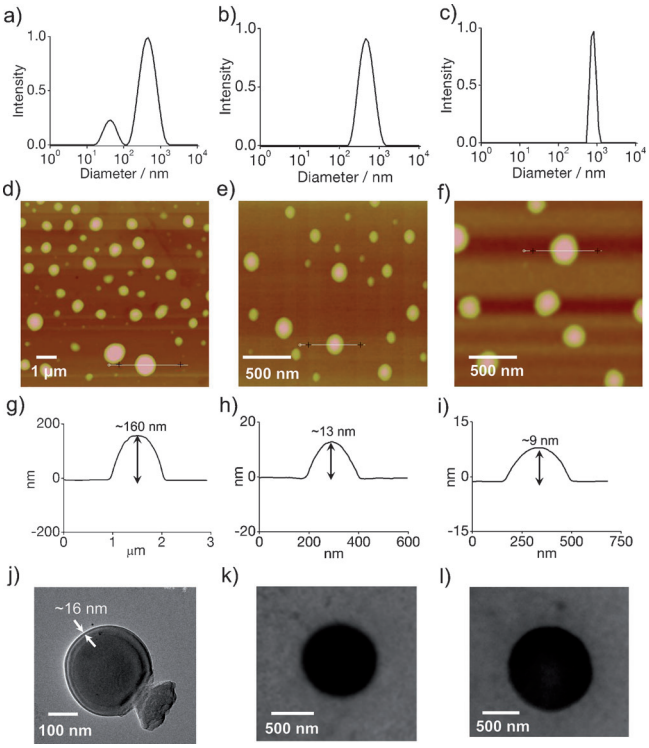

Figure 1. a–c) Size distribution from DLS measurements of a) **DNA1**, b) **DNA2**, and c) **DNA3**. d–f) AFM height images of d) **DNA1** (z-scale 200 nm), e) **DNA2** (z-scale 23 nm), and f) **DNA3** (z-scale 12 nm). g–i) Cross-section analyses of a vesicle of **DNA1–3**, respectively. j–l) TEM images of j) **DNA1**, k) **DNA2**, and l) **DNA3**. [**DNA1–3**] = 1 μM in 50 mM Tris buffer, pH 7.4.

(FE-SEM) analysis of self-assembled solutions of **DNA1–3** show the formation of spherical assemblies (SI, Figure S4–6). The height images of self-assemblies of **DNA1–3** obtained by tapping-mode atomic force microscopy (AFM) show the formation of nano- to microsized spherical assemblies (Figure 1 d–f). The average diameters of the spheres, which were estimated from the fitted histograms of the size distribution curves, are approximately 505 nm, 300 nm, and 550 nm for **DNA1–3**, respectively (SI, Figure S10). Since the observed average diameters of spheres of **DNA1–3** are much larger compared to twice the extended molecular lengths of **DNA1** (≈18 nm), **DNA2** (≈20 nm), and **DNA3** (≈21 nm), it can

be inferred that the spherical assemblies are vesicular in nature rather than simple micelles. Notably, Vesicles of **DNA1** exhibit an average height of 115 nm (Figure 1 g), whereas a drastic decrease in average height is observed for the vesicles of **DNA2** (12 nm, Figure 1 h) and **DNA3** (11 nm, Figure 1 i), much smaller than their respective average diameters. These observations clearly indicate that **DNA1** self-assembles into "hard" vesicles where complete flattening of vesicles is not expected on the surface, as proposed by Wang and Wegner et al.[21] On the other hand, the low average heights of **DNA2** and **DNA3** vesicles can be attributed to the complete flattening of the vesicles on the surface, which is a characteristic feature of "soft" vesicles. These findings were further confirmed by transmission electron microscopy (TEM) analyses. For **DNA1**, owing to their "hard" nature, the membrane of the vesicle is clearly visible with a membrane thickness of 16 nm as revealed by high resolution TEM, which is 2 nm less compared to the calculated membrane thickness of 18 nm (Figure 1 j). This difference could be attributed to the interdigitation of the alkyl chains as well as the flexible nature of single-stranded DNA (ssDNA) (Scheme 1). On the other hand, no contrast difference between the periphery and inner part of the vesicle could be seen for **DNA2** (Figure 1 k) and **DNA3** (Figure 1 l) due to their "soft" nature, and hence the membrane of the vesicles is invisible. It is also noted that no change in vesicular morphology was observed after hybridization of ssDNA on the surface of the vesicle with the corresponding complementary DNA strand (5′-TGGGTGCGAA-3′) (SI, Figure S12).

It has been generally observed for OPE-based self-assembled systems that they undergo fluorescence quenching upon aggregation.[14a,22] Interestingly, the emission intensity of OPEs in **DNA1–3** is significantly enhanced in the aggregated state compared to the corresponding monomeric amphiphiles as revealed from the temperature-dependent emission spectra. At 20 °C, vesicles of the shortest molecular wire conjugated DNA, **DNA1**, show emission of π-stacked OPEs with maximum at 408 nm ($\lambda_{ex} = 310$ nm). As expected, a gradual red-shift in emission maximum is observed for **DNA2** and **DNA3** vesicles due to the increase in conjugation of the OPE segment. **DNA2** vesicles exhibit an emission maximum at 450 nm ($\lambda_{ex} = 310$ nm), which is further red-shifted to 525 nm ($\lambda_{ex} = 320$ nm) in the case of **DNA3** vesicles. The fluorescence quantum yields for **DNA1–3** vesicles at 20 °C are 0.15, 0.1, and 0.1, respectively. Interestingly, a gradual decrease in emission intensity of OPE aggregates with the concomitant blue-shifted emission of the corresponding OPE monomer is observed upon increasing the temperature of the solutions of **DNA1–3** vesicles from 20 °C to 70 °C, in a reversible manner (Figure 2 a, c, and e, respectively). To gain more insight into the mechanism of fluorescence enhancement for the vesicles, time-resolved fluorescence studies were carried out. Decay profiles of **DNA1–3** monomers show a very fast decay with lifetime < 1 ns, indicating fast non-radiative relaxation of the excited state, and in this case, most possibly through an intramolecular C(sp^2)–C(sp) bond rotation owing to their low rotational energy barrier (ca. 0.5 kcal mol^{-1}),[23] as observed in similar systems.[24] On the other hand, significantly longer lifetimes are observed for the vesicular state of **DNA1–3** with

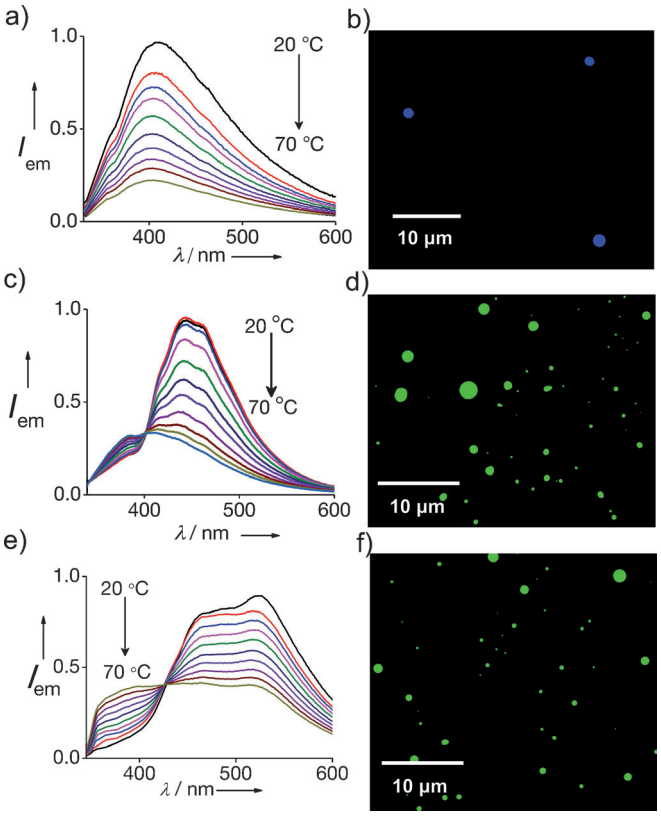

Figure 2. Temperature-dependent fluorescence spectra of a) **DNA1** ($\lambda_{ex} = 310$ nm), c) **DNA2** ($\lambda_{ex} = 310$ nm), and e) **DNA3** ($\lambda_{ex} = 320$ nm). Fluorescence microscopy ($\lambda_{ex} = 360$–370 nm) images of microvesicles of b) **DNA1**, d) **DNA2**, and f) **DNA3**. [**DNA1–3**] = 1 μM in 50 mM Tris buffer, pH 7.4.

average lifetimes 12.3 ns, 4.2 ns, and 3.9 ns, respectively (SI, Table S2). Importantly, a higher non-radiative decay rate constant ($k_{nr} = 9.80 \times 10^8\ s^{-1}$) than the radiative decay rate constant ($k_r = 0.20 \times 10^8\ s^{-1}$) is observed for **DNA1** monomers. On the other hand, in the vesicular state the non-radiative rate constant ($k_{nr} = 0.69 \times 10^8\ s^{-1}$) is significantly reduced (14.2 times lower), whereas the radiative rate constant ($k_r = 0.12 \times 10^8\ s^{-1}$) is only slightly reduced (1.7 times lower) compared to corresponding monomeric state. Similar observations were made in the case of **DNA2** and **DNA3** amphiphiles (SI, Table S3). This significant lowering of non-radiative rate constant in the case of vesicular state indicates substantial reduction of the non-radiative relaxation (intramolecular C(sp^2)–C(sp) bond rotation) of the excited state of **DNA1–3** vesicles. This results in the intramolecular planarization of the OPE backbone as evident from the red-shift in emission, and makes radiative recombination as the dominant decay channel for the excited state of the vesicles, and thereby enhances the emission (SI, Scheme S4).[25] This phenomenon of AIEE is typical for molecules having low energy barrier for intramolecular bond rotation,[26] though rigid systems are also known to exhibit AIEE.[27] In accordance with the fluorescence properties, fluorescence microscopy images show the formation of fluorescent microvesicles for **DNA1** (Figure 2 b), **DNA2** (Figure 2 d), and **DNA3** (Figure 2 f).

A remarkable feature of this class of chromophoric assembly is the DNA-directed surface addressability, which we demonstrate through surface decoration of the vesicles with 5 nm and 30 nm Au-NPs. For this purpose, surface of the Au-NPs was initially modified with a DNA sequence (dithiol-5′-TGGGTGCGAA-3′) complementary to the DNA on the surface of the vesicle, following a procedure reported by Yan and Liu et al.[28] Subsequently, assembly of **DNA1** vesicle and Au-NP (**DNA1**-vesicle–Au-NP) was prepared by annealing 1:1 molar solutions of Au-NPs (2.5 μM) and **DNA1** vesicles (2.5 μM) from 40 °C to 4 °C in 0.5 × TBE buffer containing 50 mM NaCl (T_m = 37 °C). TEM images of **DNA1**-vesicle-Au-NP (ca. 5 nm) assembly show densely packed NPs on the surface of the vesicle due to DNA hybridization (Figure 3a and b). Dense loading of NPs on the surface of the vesicles can be seen in the case of 30 nm Au-NPs as well (Figure 3c

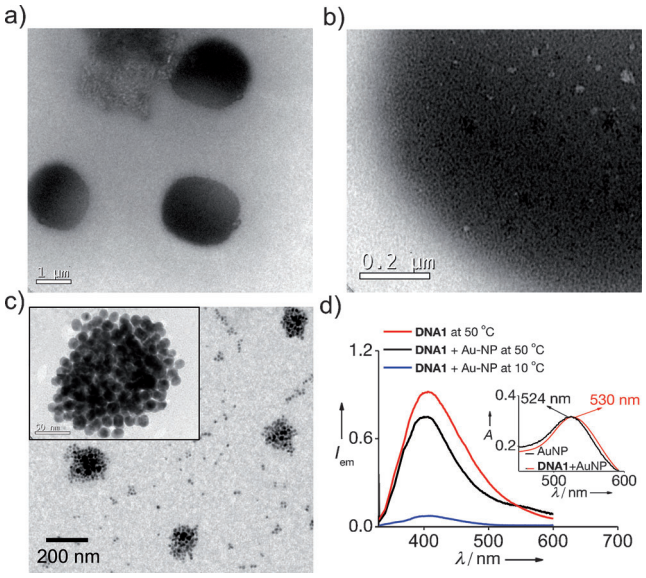

Figure 3. TEM image of a) 5 nm Au-NP decorated **DNA1 v**esicles and b) a zoomed part of a vesicle. c) TEM image of 30 nm Au-NP decorated **DNA1** vesicles; inset is a HR-TEM image of a single NP-coated vesicle. d) Fluorescence spectra of **DNA1** vesicle at 50 °C (red), 5 nm Au-NP coated **DNA1** vesicle at 50 °C (black) and 10 °C (blue); the inset shows the absorption spectrum of Au-NPs alone and after their assembly onto the vesicle surface. [**DNA1**] = 2.5 μM, [Au-NP] = 2.5 μM in 0.5 × TBE buffer, NaCl = 50 mM, pH 8.

and SI, Figures S18 and S19). Accordingly, red-shifts of 6 nm (524 nm to 530 nm) and 5 nm (525 nm to 530 nm) are respectively observed in the plasmon absorption band of 5-nm and 30-nm Au-NPs assembled on the surface of the vesicle when compared with the corresponding non-assembled NPs (Figure 3d inset and SI, Figure S20), indicating that weak interparticle surface plasmon coupling on the vesicle surface.[29] The corresponding fluorescence spectrum at 20 °C (λ_{ex} = 310 nm) shows 93 % fluorescence quenching of OPE aggregates due to their electronic interaction with Au-NPs (Figure 3d), with a Stern–Volmer quenching constant (K_{sv}) of $4.6 \times 10^6\,M^{-1}$ (SI, Figure S21).[30] This relatively high K_{sv} indicates that Au-NPs efficiently quenches the emission of **DNA1**, however, superquenching is not observed as reported in similar systems.[31] Interestingly, the fluorescence of the OPE aggregate is almost restored (81 %) upon increasing the temperature up to 50 °C due to the disassembly of the duplex, revealing the thermal reversibility of the hybrid assemblies.

Motivated by AIEE and the surface addressability of vesicles, which are promising features for the design of ideal light-harvesting system, a thermally reversible light-harvesting system with **DNA1** vesicles as a representative example is also demonstrated. We selected ethynyl perylene (SI, Scheme S2) as the acceptor in our study due to its desirable optical properties needed for a FRET pair with **DNA1** vesicle as the donor ($J(\lambda) = 4.7 \times 10^{14}\,M^{-1}\,cm^{-1}\,nm^4$). Ethynyl perylene-modified DNA (**DNA-Pe**) was synthesized on a DNA synthesizer with a sequence (5′-**Pe**-dUGGGTGCGAA-3′) complementary to the DNA on the surface of **DNA1** vesicle. Hybridization of **DNA1** vesicles and **DNA-Pe** (annealing from 40 °C to 4 °C, T_m = 37 °C) places the acceptor on the surface of the resulting assembly at a distance of ca. 5 nm from the OPE stacks (Scheme 1). Notably, the vesicular morphology of **DNA1** undergoes transition into cylindrical fibrils upon hybridization with **DNA-Pe**, as evident from AFM (Figure 4a), FE-SEM (Figure 4b), and TEM (SI, Figure S24) analyses.[12a] AFM sectional analysis reveals that the smallest fiber has a diameter of 16 nm after subtracting AFM tip-broadening,[32] and several micrometers in length (Figure 4a inset). This indicates that fibrillar assembly is cylindrical-micellar with perylene decorated on the surface as shown in Scheme 1. A very weak excimer emission of perylene is observed in the micellar assembly (SI, Figure S26).

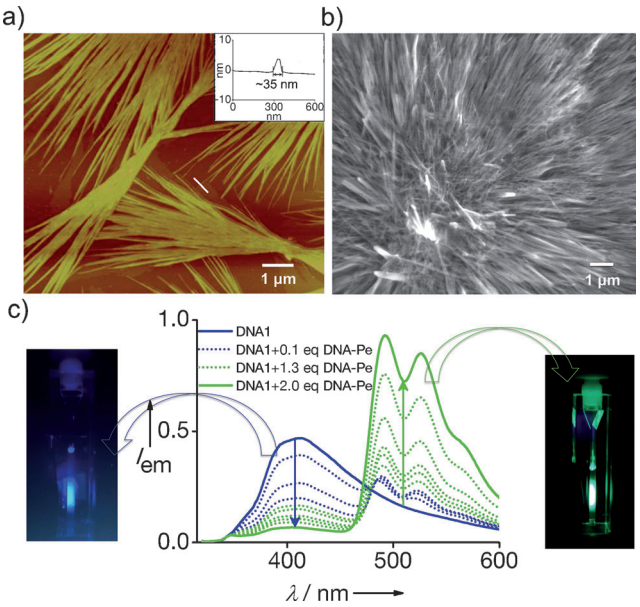

Figure 4. a) AFM height image (*z*-scale 65 nm) of **DNA1–DNA-Pe** assembly (1:1 molar). The inset shows the section analysis on a smallest fiber. b) FE-SEM image of **DNA1–DNA-Pe** assembly. c) Fluorescence spectra (λ_{ex} = 310 nm) of **DNA1** vesicle with the addition of increasing equivalence of **DNA-Pe** (up to 2 equiv). [**DNA1**] = 2.5 μM in 0.5 × TBE buffer, NaCl = 50 mM, pH 8, T = 10 °C. The corresponding emission color change of **DNA1** alone and of the **DNA1–DNA-Pe** assembly upon excitation at 310 nm is also shown.

FRET experiments were carried out ($T = 10\,^{\circ}C$) at an excitation wavelength of 310 nm where the extinction coefficient of **DNA-Pe** is relatively small ($7.0 \times 10^3\,M^{-1}cm^{-1}$) compared to **DNA1** vesicles ($1.3 \times 10^5\,M^{-1}cm^{-1}$). Gradual decrease in **DNA1** emission at 408 nm with the concomitant increase in the emission of **DNA-Pe** at 493 nm is observed upon excitation of **DNA1-DNA-Pe** assembly at 310 nm indicates the occurrence of FRET from the self-assembled OPEs of **DNA1** to **DNA-Pe** (Figure 4c). About 90% quenching of **DNA1** emission is observed upon addition of 2 equivalents of **DNA-Pe** (FRET efficiency = 85%, $k_{ET} = 1.9 \times 10^9\,s^{-1}$). Accordingly, a fluorescence microscopy image of **DNA1**-**DNA-Pe** assembly upon UV excitation ($\lambda_{ex} = 360$–370 nm) shows green emitting fibrillar structures (SI, Figure S27), which correspond to **DNA-Pe** fluorescence as a result of FRET, although the direct excitation of **DNA-Pe** cannot be completely ruled out. An interesting feature of the present light-harvesting system is the dependency of FRET efficiency on the temperature-controlled association–dissociation of the duplex. Accordingly, excitation of **DNA1**–**DNA-Pe** assembly ($\lambda_{ex} = 310$ nm) at 50 °C shows a significant decrease in the emission intensity of **DNA-Pe** with the concomitant increase in the emission intensity of **DNA1**, indicating significant decrease in the FRET efficiency upon dissociation of the duplex. Furthermore, FRET efficiency can be regained by decreasing the temperature to 20 °C, and is reversible.

In conclusion, we have demonstrated a general "click chemistry" based approach for the synthesis of DNA–OPE hybrid amphiphiles and studied their reversible self-assembly into surface-engineered vesicles with enhanced emission. This synthetic strategy can be applied to the conjugation of DNA into any class of hydrophobic chromophores for the design of new DNA–chromophore amphiphiles. The DNA-directed surface addressability of this class of chromophoric nanostructures was exploited for the reversible organization of Au-NPs and fluorophores on the surface of the vesicle. Significant electronic interaction was observed between chromophore stacks and both Au-NPs and fluorophores in the hybrid nanostructures. Since the length of the DNA duplex can be tuned by altering the number of DNA bases, this assembly offers a unique supramolecular template to study distance-dependent electronic interaction of chromophore stacks with other functional molecules. The molecular recognition properties of DNA would allow this class of surface-engineered assemblies to position them at desired location and could be a promising candidate for advancement of nanoelectronics. Our results are also expected to open up further research interest in the design of new DNA–chromophore amphiphiles for artificial light harvesting applications.

Received: March 18, 2014
Revised: May 19, 2014
Published online: June 24, 2014

Keywords: amphiphiles · chromophore · DNA nanotechnology · supramolecular chemistry · vesicles

[1] a) F. J. M. Hoeben, P. Jonkheijm, E. W. Meijer, A. P. H. J. Schenning, *Chem. Rev.* **2005**, *105*, 1491–1546; b) A. P. H. J. Schenning, E. W. Meijer, *Chem. Commun.* **2005**, 3245–3258; c) J. Wu, W. Pisula, K. Müllen, *Chem. Rev.* **2007**, *107*, 718–747; d) Z. Chen, A. Lohr, C. R. Saha-Möller, F. Würthner, *Chem. Soc. Rev.* **2009**, *38*, 564–584; e) T. M. Figueira-Duarte, K. Müllen, *Chem. Rev.* **2011**, *111*, 7260–7314; f) S. S. Babu, S. Prasanthkumar, A. Ajayaghosh, *Angew. Chem.* **2012**, *124*, 1800–1810; *Angew. Chem. Int. Ed.* **2012**, *51*, 1766–1776; g) S. Sengupta, F. Würthner, *Acc. Chem. Res.* **2013**, *46*, 2498–2512; h) K. K. Kartha, R. D. Mukhopadhyay, A. Ajayaghosh, *Chimia* **2013**, *67*, 51–63; i) S. S. Babu, V. K. Praveen, A. Ajayaghosh, *Chem. Rev.* **2014**, *114*, 1973–2129.

[2] a) F. Würthner, Z. Chen, F. J. M. Hoeben, P. Osswald, C.-C. You, P. Jonkheijm, J. v. Herrikhuyzen, A. P. H. J. Schenning, P. P. A. M. van der Schoot, E. W. Meijer, E. H. A. Beckers, S. C. J. Meskers, R. A. J. Janssen, *J. Am. Chem. Soc.* **2004**, *126*, 10611–10618; b) X. Feng, V. Marcon, W. Pisula, M. R. Hansen, J. Kirkpatrick, F. Grozema, D. Andrienko, K. Kremer, K. Müllen, *Nat. Mater.* **2009**, *8*, 421–426; c) W. Zhang, W. Jin, T. Fukushima, A. Saeki, S. Seki, T. Aida, *Science* **2011**, *334*, 340–343.

[3] N. C. Seeman, *J. Theor. Biol.* **1982**, *99*, 237–247.

[4] a) N. C. Seeman, *Nature* **2003**, *421*, 427–431; b) F. A. Aldaye, A. L. Palmer, H. F. Sleiman, *Science* **2008**, *321*, 1795–1799; c) N. C. Seeman, *Annu. Rev. Biochem.* **2010**, *79*, 65–87; d) A. V. Pinheiro, D. Han, W. M. Shih, H. Yan, *Nat. Nanotechnol.* **2011**, *6*, 763–772; e) T. Tørring, N. V. Voigt, J. Nangreave, H. Yan, K. V. Gothelf, *Chem. Soc. Rev.* **2011**, *40*, 5636–5646; f) J. Fu, M. Liu, Y. Liu, H. Yan, *Acc. Chem. Res.* **2012**, *45*, 1215–1226.

[5] a) E. T. Kool, *Acc. Chem. Res.* **2002**, *35*, 936–943; b) C. Brotschi, C. J. Leumann, *Angew. Chem.* **2003**, *115*, 1694–1697; *Angew. Chem. Int. Ed.* **2003**, *42*, 1655–1658; c) H. Kashida, H. Asanuma, M. Komiyama, *Angew. Chem.* **2004**, *116*, 6684–6687; *Angew. Chem. Int. Ed.* **2004**, *43*, 6522–6525; d) E. Mayer-Enthart, H.-A. Wagenknecht, *Angew. Chem.* **2006**, *118*, 3451–3453; *Angew. Chem. Int. Ed.* **2006**, *45*, 3372–3375; e) S. Berndl, H.-A. Wagenknecht, *Angew. Chem.* **2009**, *121*, 2454–2457; *Angew. Chem. Int. Ed.* **2009**, *48*, 2418–2421; f) R. Varghese, H.-A. Wagenknecht, *Chem. Commun.* **2009**, 2615–2624; g) R. Varghese, H.-A. Wagenknecht, *Chem. Eur. J.* **2010**, *16*, 9040–9046; h) F. Garo, R. Häner, *Angew. Chem.* **2012**, *124*, 940–943; *Angew. Chem. Int. Ed.* **2012**, *51*, 916–919.

[6] a) K. C. Hannah, B. A. Armitage, *Acc. Chem. Res.* **2004**, *37*, 845–853; b) R. Iwaura, F. J. M. Hoeben, M. Masuda, A. P. H. J. Schenning, E. W. Meijer, T. Shimizu, *J. Am. Chem. Soc.* **2006**, *128*, 13298–13304; c) P. G. A. Janssen, J. Vandenbergh, J. L. J. van Dongen, E. W. Meijer, A. P. H. J. Schenning, *J. Am. Chem. Soc.* **2007**, *129*, 6078–6079; d) S. Sezi, H.-A. Wagenknecht, *Chem. Commun.* **2013**, *49*, 9257–9259.

[7] M. Kwak, A. Herrmann, *Angew. Chem.* **2010**, *122*, 8754–8768; *Angew. Chem. Int. Ed.* **2010**, *49*, 8574–8587.

[8] a) F. E. Alemdaroglu, N. C. Alemdaroglu, P. Langguth, A. Herrmann, *Adv. Mater.* **2008**, *20*, 899–902; b) M. Kwak, I. J. Minten, D.-M. Anaya, A. J. Musser, M. Brasch, R. J. M. Nolte, K. Müllen, J. J. L. M. Cornelissen, A. Herrmann, *J. Am. Chem. Soc.* **2010**, *132*, 7834–7835; c) A. M. Rush, M. P. Thompson, E. T. Tatro, N. C. Gianneschi, *ACS Nano* **2013**, *7*, 1379–1387; d) T. Chen, C. S. Wu, E. Jimenez, Z. Zhu, J. G. Dajac, M. You, D. Han, X. Zhang, W. Tan, *Angew. Chem.* **2013**, *125*, 2066–2070; *Angew. Chem. Int. Ed.* **2013**, *52*, 2012–2016.

[9] a) M. Kwak, J. Gao, D. K. Prusty, A. J. Musser, V. A. Markov, N. Tombros, M. C. A. Stuart, W. R. Browne, E. J. Boekema, G. ten Brinke, H. T. Jonkman, B. J. van Wees, M. A. Loi, A. Herrmann, *Angew. Chem.* **2011**, *123*, 3264–3268; *Angew.*

Chem. Int. Ed. **2011**, *50*, 3206 – 3210; b) M.-P. Chien, N. C. Gianneschi, *Small* **2011**, *7*, 2041 – 2046.

[10] a) Z. Li, Y. Zhang, P. Fullhart, C. A. Mirkin, *Nano Lett.* **2004**, *4*, 1055 – 1058; b) F. E. Alemdaroglu, K. Ding, R. Berger, A. Herrmann, *Angew. Chem.* **2006**, *118*, 4313 – 4317; *Angew. Chem. Int. Ed.* **2006**, *45*, 4206 – 4210; c) M.-P. Chien, A. M. Rush, M. P. Thompson, N. C. Gianneschi, *Angew. Chem.* **2010**, *122*, 5202 – 5206; *Angew. Chem. Int. Ed.* **2010**, *49*, 5076 – 5080; d) Z. Zhao, L. Wang, Y. Liu, Z. Yang, Y.-M. He, Z. Li, Q.-H. Fan, D. Liu, *Chem. Commun.* **2012**, *48*, 9753 – 9755; e) S. E. Averick, S. K. Dey, D. Grahacharya, K. Matyjaszewski, S. R. Das, *Angew. Chem.* **2014**, *126*, 2777 – 2782; *Angew. Chem. Int. Ed.* **2014**, *53*, 2739 – 2744.

[11] a) K. M. M. Carneiro, F. A. Aldaye, H. F. Sleiman, *J. Am. Chem. Soc.* **2010**, *132*, 679 – 685; b) L. Wang, Y. Feng, Y. Sun, Z. Li, Z. Yang, Y.-M. He, Q.-Hua Fan, D. Liu, *Soft Matter* **2011**, *7*, 7187 – 7190; c) T. G. W. Edwardson, K. M. M. Carneiro, C. K. McLaughlin, C. J. Serpell, H. F. Sleiman, *Nat. Chem.* **2013**, *5*, 868 – 875; d) Y. Dong, Y. Sun, L. Wang, D. Wang, T. Zhou, Z. Yang, Z. Chen, Q. Wang, Q. Fan, D. Liu, *Angew. Chem.* **2014**, *126*, 2645 – 2648; *Angew. Chem. Int. Ed.* **2014**, *53*, 2607 – 2610.

[12] a) M. P. Thompson, M.-P. Chien, T.-H. Ku, A. M. Rush, N. C. Gianneschi, *Nano Lett.* **2010**, *10*, 2690 – 2693; b) M. Anaya, M. Kwak, A. J. Musser, K. Müllen, A. Herrmann, *Chem. Eur. J.* **2010**, *16*, 12852 – 12859.

[13] H. Liu, Z. Zhu, H. Kang, Y. Wu, K. Sefan, W. Tan, *Chem. Eur. J.* **2010**, *16*, 3791 – 3797.

[14] a) A. Ajayaghosh, R. Varghese, V. K. Praveen, S. Mahesh, *Angew. Chem.* **2006**, *118*, 3339 – 3342; *Angew. Chem. Int. Ed.* **2006**, *45*, 3261 – 3264; b) A. Ajayaghosh, R. Varghese, S. Mahesh, V. K. Praveen, *Angew. Chem.* **2006**, *118*, 7893 – 7896; *Angew. Chem. Int. Ed.* **2006**, *45*, 7729 – 7732; c) S. Yagai, S. Mahesh, Y. Kikkawa, K. Unoike, T. Karatsu, A. Kitamura, A. Ajayaghosh, *Angew. Chem.* **2008**, *120*, 4769 – 4772; *Angew. Chem. Int. Ed.* **2008**, *47*, 4691 – 4694; d) S. Mahesh, R. Thirumalai, S. Yagai, A. Kitamura, A. Ajayaghosh, *Chem. Commun.* **2009**, 5984 – 5986.

[15] a) C. S. Andersen, H. Yan, K. V. Gothelf, *Angew. Chem.* **2008**, *120*, 5651 – 5654; *Angew. Chem. Int. Ed.* **2008**, *47*, 5569 – 5572; b) C. S. Andersen, M. M. Knudsen, R. Chhabra, Y. Liu, H. Yan, K. V. Gothelf, *Bioconjugate Chem.* **2009**, *20*, 1538 – 1546.

[16] a) K. V. Gothelf, A. Thomsen, M. Nielsen, E. Cló, R. S. Brown, *J. Am. Chem. Soc.* **2004**, *126*, 1044 – 1046; b) M. Nielsen, A. H. Thomsen, E. Cl, F. Kirpekar, K. V. Gothelf, *J. Org. Chem.* **2004**, *69*, 2240 – 2250; c) P. Blakskjær, K. V. Gothelf, *Org. Biomol. Chem.* **2006**, *4*, 3442 – 3447; d) J. B. Ravnsbæk, M. F. Jacobsen, C. B. Rosen, N. V. Voigt, K. V. Gothelf, *Angew. Chem.* **2011**, *123*, 11043 – 11046; *Angew. Chem. Int. Ed.* **2011**, *50*, 10851 – 10854.

[17] I. Eryazici, T. R. Prytkova, G. C. Schatz, S. T. Nguyen, *J. Am. Chem. Soc.* **2010**, *132*, 17068 – 17070.

[18] C. J. Yang, M. Pinto, K. Schanze, W. Tan, *Angew. Chem.* **2005**, *117*, 2628 – 2632; *Angew. Chem. Int. Ed.* **2005**, *44*, 2572 – 2576.

[19] a) J. Gierlich, G. A. Burley, P. M. E. Gramlich, D. M. Hammond, T. Carell, *Org. Lett.* **2006**, *8*, 3639 – 3642; b) A. H. El-Sagheerab, T. Brown, *Chem. Soc. Rev.* **2010**, *39*, 1388 – 1405; c) C. Beyer, H.-A. Wagenknecht, *Chem. Commun.* **2010**, *46*, 2230 – 2231; d) S. Pal, R. Varghese, Z. Deng, Z. Zhao, A. Kumar, H. Yan, Y. Liu, *Angew. Chem.* **2011**, *123*, 4262 – 4265; *Angew. Chem. Int. Ed.* **2011**, *50*, 4176 – 4179.

[20] a) A. J. Wilson, M. Masuda, R. P. Sijbesma, E. W. Meijer, *Angew. Chem.* **2005**, *117*, 2315 – 2319; *Angew. Chem. Int. Ed.* **2005**, *44*, 2275 – 2279; b) A. Lohr, M. Lysetska, F. Würthner, *Angew. Chem.* **2005**, *117*, 5199 – 5202; *Angew. Chem. Int. Ed.* **2005**, *44*, 5071 – 5074; c) S. Yagai, K. Iwai, T. Karatsu, A. Kitamura, *Angew. Chem.* **2012**, *124*, 9817 – 9821; *Angew. Chem. Int. Ed.* **2012**, *51*, 9679 – 9683; d) S. Yagai, M. Yamauchi, A. Kobayashi, T. Karatsu, A. Kitamura, T. Ohba, Y. Kikkawa, *J. Am. Chem. Soc.* **2012**, *134*, 18205 – 18208.

[21] M. Yang, W. Wang, F. Yuan, X. Zhang, J. Li, F. Liang, B. He, B. Minch, G. Wegner, *J. Am. Chem. Soc.* **2005**, *127*, 15107 – 15111.

[22] J. Kim, I. A. Levitsky, D. T. McQuade, T. M. Swager, *J. Am. Chem. Soc.* **2002**, *124*, 7710 – 7718.

[23] M. Levitus, K. Schmieder, H. Ricks, K. D. Shimizu, U. H. F. Bunz, M. A. Garcia-Garibay, *J. Am. Chem. Soc.* **2001**, *123*, 4259 – 4265.

[24] S.-J. Yoon, J. H. Kim, K. S. Kim, J. W. Chung, B. Heinrich, F. Mathevet, P. Kim, B. Donnio, A.-J. Attias, D. Kim, S. Y. Park, *Adv. Funct. Mater.* **2012**, *22*, 61 – 69.

[25] Y. Tang, Z. Zhou, K. Ogawa, G. P. Lopez, K. S. Schanze, D. G. Whitten, *Langmuir* **2009**, *25*, 21 – 25.

[26] Y. Hong, J. W. Y. Lam, B. Z. Tang, *Chem. Soc. Rev.* **2011**, *40*, 5361 – 5388.

[27] X. Zhang, D. Görl, V. Stepanenko, F. Würthner, *Angew. Chem.* **2014**, *126*, 1294 – 1298; *Angew. Chem. Int. Ed.* **2014**, *53*, 1270 – 1274.

[28] J. Sharma, R. Chhabra, C. S. Andersen, K. V. Gothelf, H. Yan, Y. Liu, *J. Am. Chem. Soc.* **2008**, *130*, 7820 – 7821.

[29] B. Ding, Z. Deng, H. Yan, S. Cabrini, R. N. Zuckermann, J. Bokor, *J. Am. Chem. Soc.* **2010**, *132*, 3248 – 3249.

[30] J. van Herrikhuyzen, S. J. George, M. R. J. Vos, N. A. J. M. Sommerdijk, A. Ajayaghosh, S. C. J. Meskers, A. P. H. J. Schenning, *Angew. Chem.* **2007**, *119*, 1857 – 1860; *Angew. Chem. Int. Ed.* **2007**, *46*, 1825 – 1828.

[31] C. Fan, S. Wang, J. W. Hong, G. C. Bazan, K. W. Plaxco, A. J. Heeger, *Proc. Natl. Acad. Sci. USA* **2003**, *100*, 6297 – 6301.

[32] P. Samorí, V. Francke, T. Mange, K. Müllen, J. P. Rabe, *Opt. Mater.* **1998**, *9*, 390 – 393.

